Ceramics International 32 (2006) 891–897

CERAMICS INTERNATIONAL

www.elsevier.com/locate/ceramint

Production of β-SiC by pyrolysis of rice husk in gas furnaces

V. Martínez [a,*], M.F. Valencia [b], J. Cruz [a], J.M. Mejía [c], F. Chejne [c]

[a] *GINUMA, Universidad Pontificia Bolivariana, A.A. 56006 Medellín, Colombia*

[b] *Escuela de Ingeniería de Antioquia, A.A. 7516 Medellín, Colombia*

[c] *Instituto de Energía, Facultad de Mínas, Universidad Nacional de Colombia, A.A. 568 Medellín, Colombia*

Received 13 January 2005; received in revised form 30 March 2005; accepted 2 July 2005

Abstract

Short fibers and fine particles of β-SiC were obtained by pyrolysis of Colombian rice husk (RH). The synthesis of SiC was carried out in a gas furnace: a mathematical model was developed in order to design and build this equipment and the process was optimized using an experimental design that included variables such as temperature, pyrolysis time, type of catalyst, and process atmosphere. The obtained material was characterized by using FTIR, DRX and SEM for microstructural characterization and EDS technique for chemical analysis.

Keywords: A. Calcination; B. Electron microscopy; D. SiC; DRX; Experimental design

1. Introduction

Carbides are widely recognized as materials with high mechanical wear resistance, hardness, and thermal and chemical stability within the set of modern ceramics [1]. Among the non-oxide ceramics, silicon carbide can be produced like fibers or whiskers using various thermo-chemical processes [2]. Two of the main methods employed are (i) the mixing of silica with carbon in the presence of inert gas at temperatures between 1300 and 1500 °C [3]; and (ii) the mixing of silica and carbon by heating of coal and silica in an atmosphere of chlorhydric or fluorhydric acid at temperatures between 1300 and 1550 °C [4]. On the other hand, it is widely known that rice husk (RH) contains more than 90% of silica and that from a controlled thermal decomposition process (pyrolysis), it is easy to obtain SiC as fine particles or whisker shapes, with diameters between 0.5 and 1 μm and lengths between 10 and 80 μm [5,6]. This alternative is useful because this process is carried out with an agro-industrial remainder, diminishing the environmental impact and therefore the costs. In the particular case of β-SiC, the processes to obtain fibers and particles are expensive; these consist conventionally in the use of CVD and VLS techniques in electrical furnaces [7].

The goal of this paper is to present a new process for production SiC-based materials. Firstly, it was necessary to prepare the RH before the process of thermal decomposition. This preparation consists of the sweepings elimination, size classification by sifting and the use of catalysts to increase the efficiency of the process [8]. The effects of two different catalysts were investigated ($CoCl_2 \cdot 6H_2O$ and $FeCl_2 \cdot 4H_2O$ with NH_4OH as a Fe precipitation agent). The catalysts decrease the activation energy required for the reagents in order to convert them into products, increasing the reaction rate, silica production, as well as decreasing the temperature of the reaction [9].

Secondly, a controlled pyrolysis process of RH has been developed. The products separation was done after the RH pyrolysis. The SiC can be separated by flotation techniques [10]; however, ultra fine solid particles tend to adhere to heavier particles. In this study, the separation process was performed pneumatically by means of cyclone separator equipment.

2. Pyrolysis equipment design

The common equipments for thermal decomposition of the RH are electrical furnaces. The energy consumption and cost associated with these equipments are high, because it is necessary to get elevated temperatures to be handled during the last pyrolysis stages. In this sense, the use of gaseous fuels

---

* Corresponding author. Tel.: +57 4 4159095; fax: +57 4 4112372.
E-mail address: hadervm@upb.edu.co (V. Martínez).

0272-8842/$30.00 © 2005 Elsevier Ltd and Techna Group S.r.l. All rights reserved.
doi:10.1016/j.ceramint.2005.07.018

Nomenclature

A	suface area (m^2)
Cp	heat capacity at constant pressure for the gas i ($kJ\ kg^{-1}\ K$)
e	excess air
F	gas flow ($kg\ s^{-1}$)
ΔfH_i°	enthalpy of formation of species i ($kJ\ kg^{-1}$)
h_M	coefficient of heat transfer between the flame (hot gases) and the sample ($kW\ m^{-2}\ K^{-1}$)
h_w	coefficient of heat transfer between gases and walls ($kW\ m^{-2}\ K^{-1}$)
h_∞	coefficient of heat transfer between external wall of furnace and the surroundings ($kW\ m^{-2}\ K^{-1}$)
k	conductivity ($kW\ m^{-2}$)
m	mass (kg)
M	molecular mass ($kg\ kmol^{-1}$)
T	temperature (K)
V	volume of combustion chamber (m^3)

Subscripts

CO_2	carbon dioxide
C_3H_8	propane
H_2O	water
in	input
ins	insulation
LL	flame
N_2	nitrogen
O_2	oxygen
ref	reference
w	wall
x = int	position, indicate the internal wall of the furnace
x = ext	position, indicate the external wall of the furnace

Greek symbols

α	diffusivity ($m^2\ s^{-1}$)
ρ	density of gases ($kg\ m^{-3}$)

(propane) offer excellent possibilities because of the high calorific power of this fuel and of its low cost. The main problem with high temperature, pressure, and low residence time operations is the prediction of the heat flux profiles on the pyrolysis furnace tube walls, where the tube skin temperature becomes the limiting factor [11]. In order to predict the RH temperature evolution, a mathematical model for a one-dimensional time dependent system was proposed. This model considers the propane combustion with excess air and the energy lost through the furnace walls (Fig. 1).

2.1. Combustion reaction and global energy balance

The combustion reaction considered is given by (1):

$$\begin{aligned} C_3H_8 + 5(1+e)(O_2 + 3.76N_2) &\rightarrow 3CO_2 + 4H_2O \\ &+ 5(1+e)3.76N_2 + 5eO_2 \end{aligned} \tag{1}$$

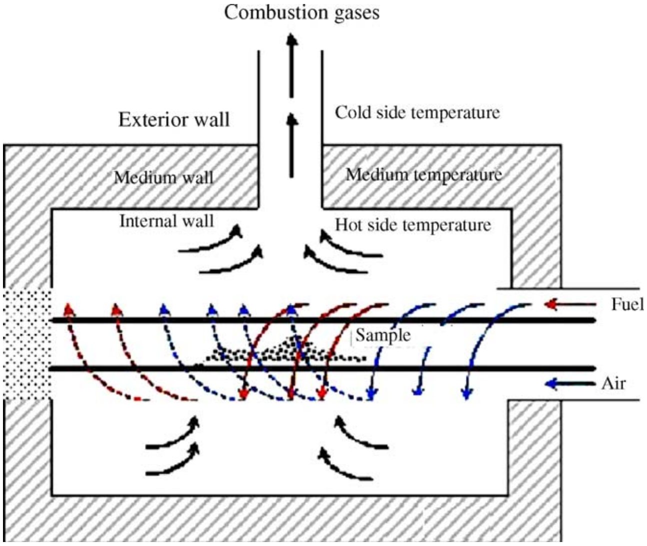

Fig. 1. Operational scheme for the pyrolysis equipment.

According to (1), the final combustion products are predicted assuming a total combustion process. This hypothesis is valid in this case, where the interest is the energy interchanges and not the pollution emissions during the process.

The global energy balance in a transient state (2), accounts for the combustion energy, energy transferred among combustion gases, internal walls, the sample, and finally the energy stored in the gases:

$$\begin{aligned} &\frac{F}{M_{C_3H_8}}\Delta fH^\circ_{C_3H_8} + 5(1+e)\frac{F}{M_{C_3H_8}}Cp_{O_2}(T_e - T_{ref}) + 5 \\ &\quad\times 3.76(1+e)\frac{F_{GN}}{M_{C_3H_8}}Cp_{N_2}(T_{in} - T_{ref}) \\ &= 3\frac{F}{M_{C_3H_8}}\left[\int_{T_{ref}}^{T_{LL}} Cp_{CO_2}\,dT + \Delta fH^\circ_{CO_2}\right] \\ &\quad + 4\frac{F_{GN}}{M_{C_3H_8}}\left[\int_{T_{ref}}^{T_{LL}} Cp_{H_2O}\,dT + \Delta fH^\circ_{H_2O}\right] + 5e \\ &\quad\times \frac{F}{M_{C_3H_8}}\int_{T_{ref}}^{T_{LL}} Cp_{O_2}\,dT + 5 \\ &\quad\times 3.76(1+e)\frac{F}{M_{C_3H_8}}\int_{T_{ref}}^{T_{LL}} Cp_{N_2}\,dT + h_M A_M(T_{LL} - T_M) \\ &\quad + h_M A_M(T_{LL} - T_M) + h_w A_w(T_{LL} - T_w) + \rho V Cp_{LL}\frac{dT_{LL}}{dt} \end{aligned} \tag{2}$$

From Eqs. (1) and (2), the flame temperature can be determined considering simultaneously the energy released during the oxidation process and the energy interchanges with the surrounding systems (sample and internal walls).

2.2. Rice husk heating

Eq. (3) gives the energy exchange from combustion gases at T_{LL} to the sample a T_M, which is calculated from the energy from the hot gases and the energy stored through the process:

$$h_{\mathrm{M}}A_{\mathrm{M}}(T_{\mathrm{LL}}-T_{\mathrm{M}})=m_{\mathrm{M}}\mathrm{Cp}_{\mathrm{M}}\frac{\mathrm{d}T_{\mathrm{M}}}{\mathrm{d}t} \tag{3}$$

The energy transferred from combustion gases to the internal walls of the furnace, Eq. (4), is simulated considering the energy from hot gases and the heat conduction through the internal wall in the pyrolysis equipment:

$$h_{\mathrm{w}}A_{\mathrm{w}}(T_{\mathrm{LL}}-(T_{\mathrm{w}})_{x=\mathrm{int}})=k_{\mathrm{w}}A_{\mathrm{w}}\left[\frac{\partial T_{\mathrm{w}}}{\partial x}\right]_{x=\mathrm{int}} \tag{4}$$

This last equation is also a boundary condition for Eq. (5), which models the heat transference through the furnace's walls:

$$\frac{\partial^2 T_{\mathrm{w}}}{\partial x^2}=\frac{1}{\alpha_{\mathrm{ins}}}\frac{\partial T_{\mathrm{w}}}{\partial t} \tag{5}$$

Finally, the second border condition that is required in order to complete the model is shown in (6). This is the convection heat transference between the external walls and the surroundings:

$$h_{\infty}A_{\mathrm{w}}\left(T_{\mathrm{w}}\Big|_{x=\mathrm{ext}}\right)=k_{\mathrm{w}}A_{\mathrm{w}}\left[\frac{\partial T_{\mathrm{w}}}{\partial x}\right]_{x=\mathrm{ext}} \tag{6}$$

Eqs. (1)–(6) enable modeling profile flame temperature evolution, the temperature of the sample and the temperature profile inside the furnace walls (Fig. 2). Fig. 3 shows both the calculated temperature and the experimental values. It can be noted that the mathematical model predicts that the maximum operation temperature (1500 °C) is reached in 300 min in accordance with experimental results. The measured temperature evolution at the beginning of the process is faster than the model predictions. This indicates that the heat losses towards the atmosphere are smaller than the one assumed by the model. These results were useful in order to perform the construction of the pyrolysis equipment (Fig. 4).

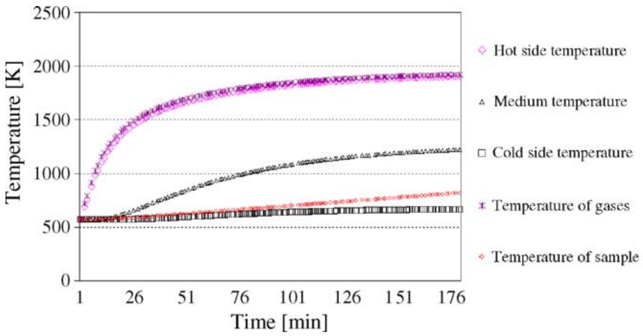

Fig. 2. Evolution of theoretical temperatures using mathematical simulation (see Fig. 1).

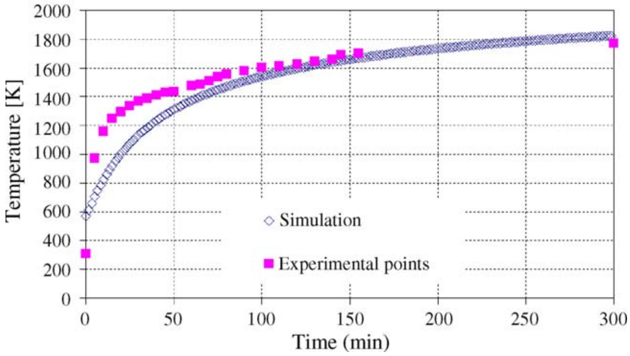

Fig. 3. Evolution of the temperature of the HR during the thermal decomposition by pyrolysis.

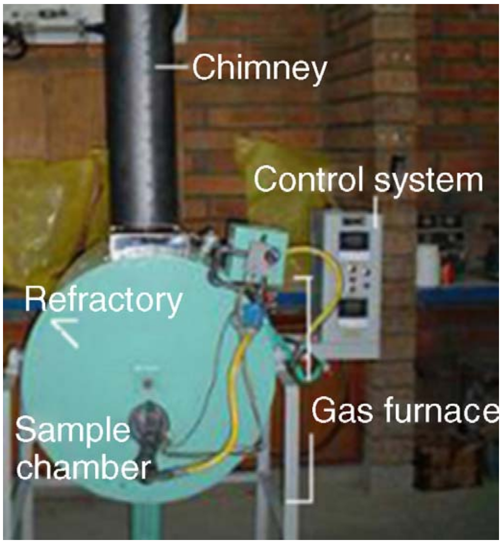

Fig. 4. Rice husk pyrolysis equipment.

3. Rice husk characterization

The Colombian rice husk used for the SiC production is known as Paddy Fedearroz 50. The atomic absorption analysis of this material, showed: 70.9% SiO_2 (from 12.07% of remainders) and 33.15% Si (from 70.9% of SiO_2). The ash contained in the used rice's husk (~12.07%) (Fig. 5), is within the inferior percentages limits determined at a worldwide level. The ash content depends on diverse factors, like ground, climate and fertilizers. In general, minor ash contents are beneficial for a greater production of SiC [12]. Finally, the organic carbon content found (43.6%) is the same reported by others researchers [13,14].

The thermogravimetric analysis in Fig. 5 shows loss of the hygroscopic water between 96 and 150 °C, and loss of volatile organic matter between 300 and 420 °C. The combustion of the solid organic matter, with a possible liberation of volatile in smaller scale, begins approximately from 420 °C.

On the other hand, the chemical analysis (see Table 1), confirms the results of Krishnarao et al. [14], where the Fe and Co contents in RH without catalyzing are minimum. Unlike, in RH catalyzed samples, Fe and Co contents considerably increases, which allow then during the pyrolysis, to reach

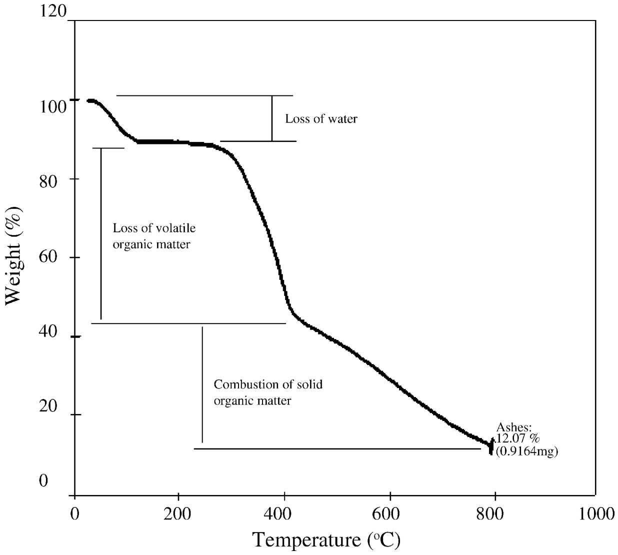

Fig. 5. Thermogravimetry of a RH sample.

Table 1
Chemical analysis of the RH

RH	Mass (g)	Co (ppm)	Fe (wt.%)
Crude	2.0218	4.85	–
Catalyzed with $CoCl_2 \cdot 6H_2O$	2.0368	524.10	–
Crude	2.0126	–	0.132
Catalyzed with $FeCl_2 \cdot 4H_2O$	2.0057	–	0.383

shorter times and temperatures for SiC production [15,16]. The chemical analysis was carried out in an atomic absorption spectrometer (UNICAM 929 AA Spectrometer- wavelength of 248.3 and 240.7 nm).

4. Ashes characterization

4.1. FTIR

The FTIR analysis was performed in a Perking-Elmer RX equipment. The spectrum of catalyzed samples with $FeCl_2 \cdot 4H_2O$

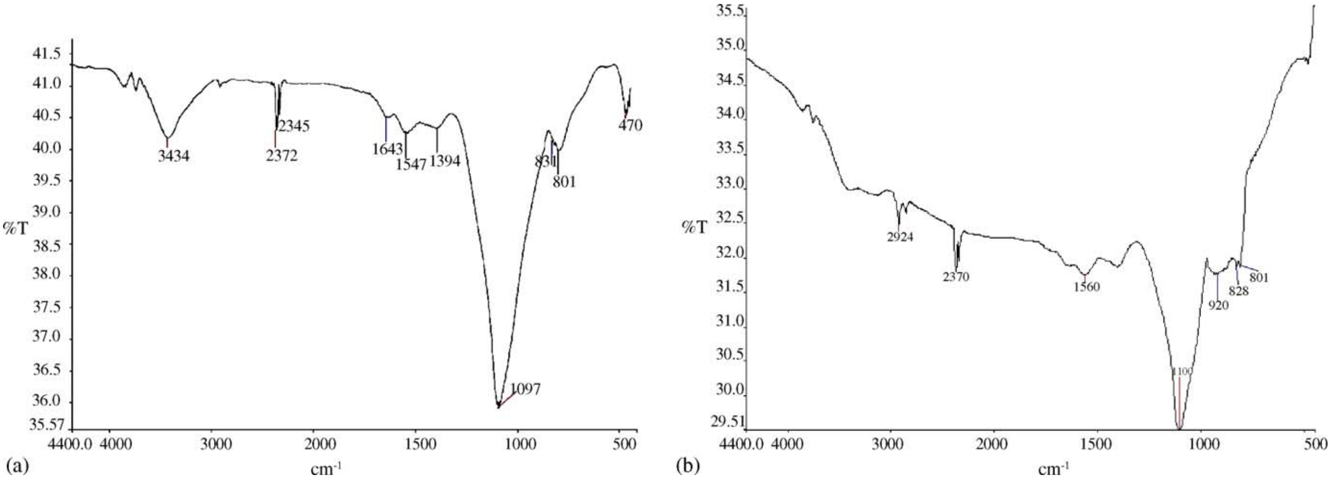

Fig. 6. FTIR spectra of catalyzed SiC ashes with: (a) $FeCl_2 \cdot 4H_2O$, (b) $CoCl_2 \cdot 6H_2O$.

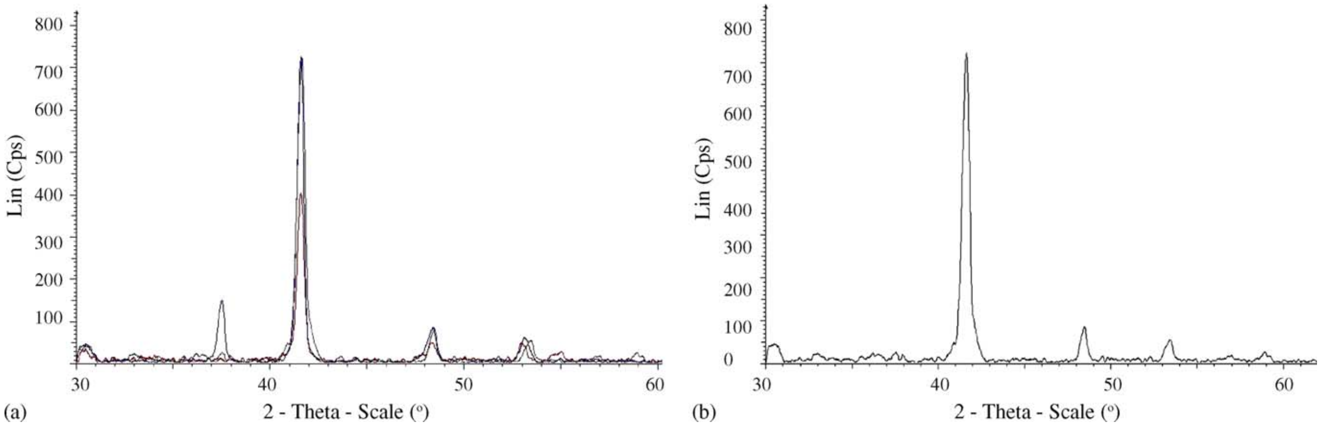

Fig. 7. DRX of catalyzed SiC ashes with: (a) $FeCl_2 \cdot 4H_2O$, (b) $CoCl_2 \cdot 6H_2O$ (Lin: linear scale, cps: counts per second).

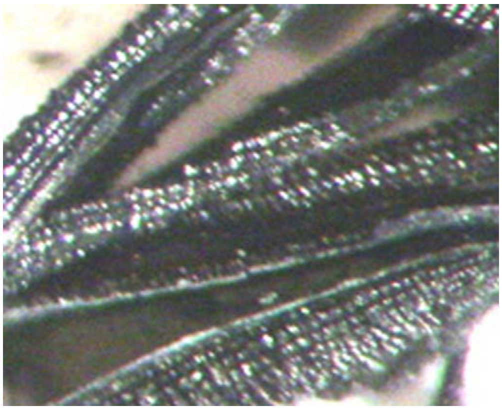

Fig. 8. Macroscopic image of calcined husk without milling (10×).

(Fig. 6a), is in accordance with the theoretical results, e.g. [17]; there are similarities in the tips around 1100 cm^{-1}, which corresponds to the group Si–O. On the other hand, the spectra of catalyzed samples with $CoCl_2 \cdot 4H_2O$ (Fig. 6b), exhibits a wide signal around 800 cm^{-1}, wave value in which the carbon–silicon extension band is reported in the literature [12]. In addition to this band, it can also be observed an absorption band approximately at 1280 cm^{-1}, which is characteristic of siloxanes groups (Si–O–Si).

4.2. X-ray diffraction

This analysis was executed in a Bruker D8-Advance dust equipment with Fe filter, K-α of Co ($\lambda_{Co} = 1.78897$ Å) and

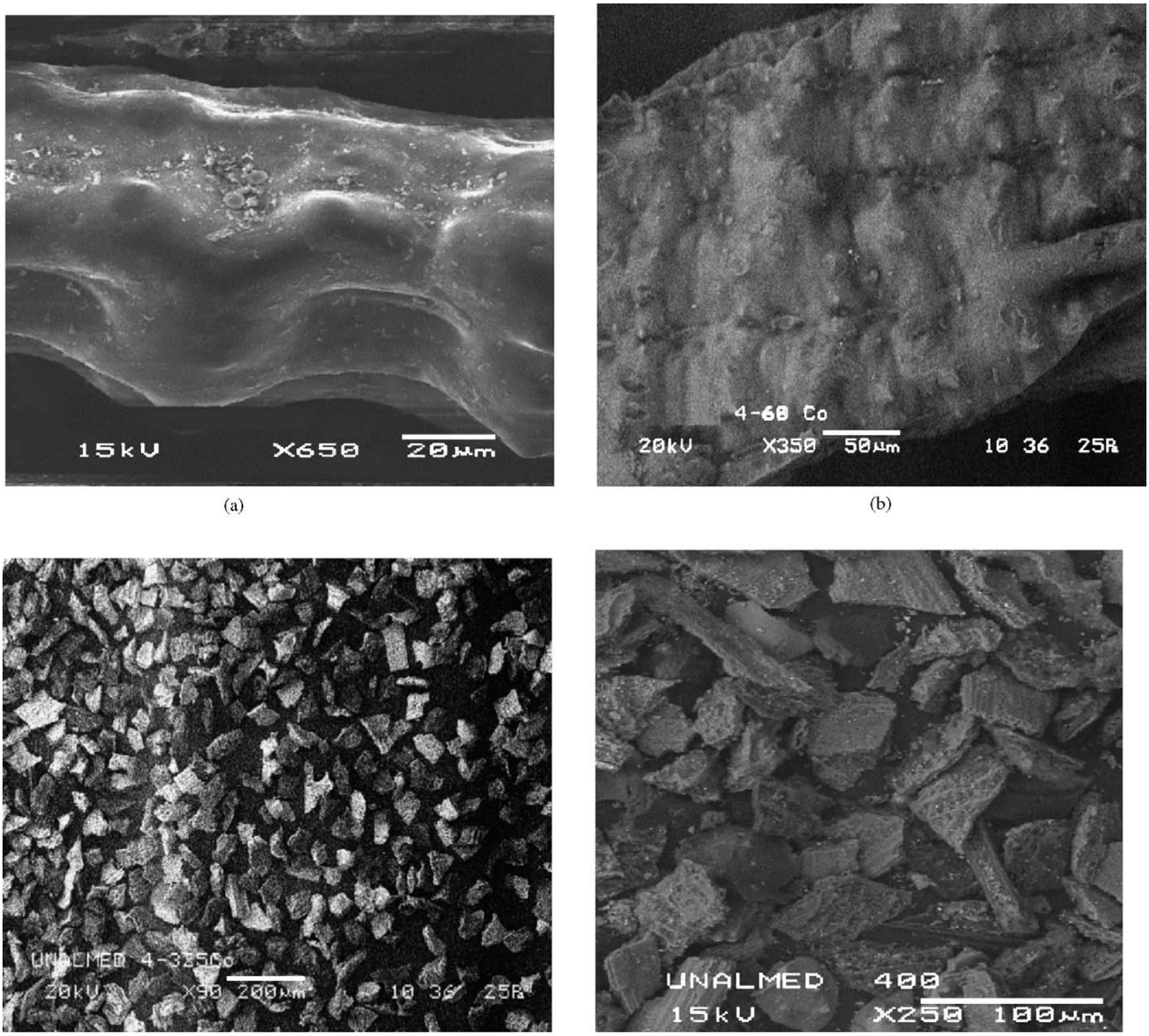

(a) (b)

(c) (d)

Fig. 9. SEM of catalyzed β-SiC ashes with: (a) $FeCl_2 \cdot 4H_2O$ (150 µm), (b) $CoCl_2 \cdot 6H_2O$ (250 µm), (c) $CoCl_2 \cdot 6H_2O$ (45 µm), (d) $FeCl_2 \cdot 4H_2O$ (38 µm).

position sensible detection. The diffractograms, indexed with PDFM phase data base, shown high intensity values at 41.575° and 48.395°. The DRX for ash catalyzed with $FeCl_2 \cdot 4H_2O$ (Fig. 7a) shows high intensity tips at different 2θ according to the theoretical data base elements that had been used. Similarly, for ashes catalyzed with $CoCl_2 \cdot 6H_2O$, there are also good results (Fig. 7b), indicating the presence of SiC crystals. DRX theoretical results for RH pyrolysis reports the formation of β-SiC at working temperatures between 1050 and 1400 °C, argon flow of $0.1\ l\ min^{-1}$ and process time between 1 and 8 h maximum [16,18,19]. For the case studied, the β-SiC crystals are obtained in smaller times, which is a consequence of the catalysts use.

4.3. Microstructural observation and EDS analysis

The macrograph shown in Fig. 8 was obtained using an Olympus SZ-PT optical microscope; the brightness in some parts is probably caused by the presence of silica. The macroscopic observation for blackened husk does not show a great difference before and after the pyrolysis. However, the amount of pores in the blackened husk is remarkable. The β-SiC ashes showed a grain sized distribution from mesh 38 to 250 μm. The heavier ashes (125–250 μm) showed short fiber forms (Fig. 9a and b), made by structures with undulating and spongy contours with 60 μm separation which are useful for the processing of metal matrix composites [20]. The fine ashes (<53 μm) showed equiaxial forms (Fig. 9c and d).

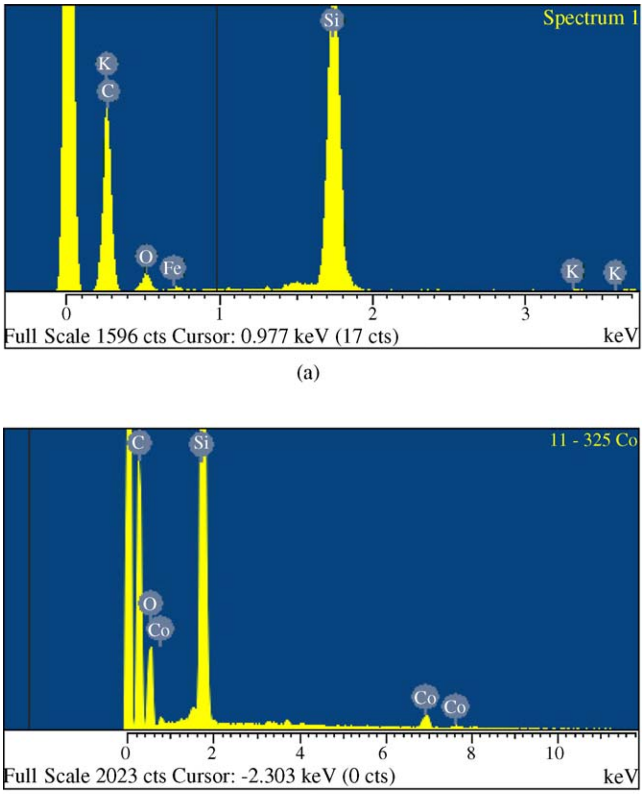

(a)

(b)

Fig. 10. EDS spectrum of catalyzed β-SiC ashes with: (a) $FeCl_2 \cdot 4H_2O$, (b) $CoCl_2 \cdot 6H_2O$.

Finally, the semi-quantitative analyses by EDS are shown in Fig. 10, where the main constitutive elements and impurities that remain after the pyrolysis can be found. The catalyzed ashes are mainly compounds of C and Si, and the Fe and the Co appear because of the catalyst employed.

5. Result of the experimental design

A Taguchi [21] experimental design was followed in this research. In this sense, the matrix that has been used is the type $L_{16}4^5$ of 16 experiments. The selected answer variable is the purity of obtained SiC, which is described by means of the crystallinity in DRX tests. According to experimental design, the best conditions processes were: 1370 °C, $1.5\ l\ min^{-1}$ argon flow, a residence time of 40 min, size of 2.36 mm for the RH and $FeCl_2 \cdot 4H_2O$ catalyzer.

6. Conclusions

β-SiC has been obtained by pyrolysis of rice husk in a gas furnace. The mathematical model used to predict the temperature evolution during the thermal decomposition and for the furnace design showed a good agreement with experimental measurements. From an experimental design, the optimized production process was developed using as a $FeCl_2 \cdot 4H_2O$ catalyzer, 1370 °C as process temperature, $1.5\ l\ min^{-1}$ argon flow and 40 min residence time. In this way, alternative uses for the rice husk are generated as new products that are manufactured from a remainder material.

Acknowledgement

Support from COLCIENCIAS under grant no. 1210-08-12545 is gratefully acknowledged.

References

[1] L.Y. Sun, K.C. Gong, Silicon based materials from rice husk and their applications, Industrial & Engineering Chemistry Research, J. Am. Chem. Soc. 40 (2001) 5861–5877.
[2] P.C. Silva, J.L. Figueiredo, Production of SiC and Si_3N_4 whiskers in $C+SiO_2$ solid mixtures, Mater. Chem. Phys. 72 (2001) 326–331.
[3] C. Jair, C. Freitas, J.S. Moreira, F.G. Emmerich, T.J. Bonagamba, Development of Si/C/N/O ceramics from pyrolyzed and heat-treated rice hulls, J. Non-Cryst. Solids 341 (2004) 77–85.
[4] W.W. Pultz, U.S. patent 3 371 995, 5, 1968.
[5] K. Othmer, Encyclopedia of Chemical Technology, USA, 1992.
[6] G. Padmaja, P.G. Mukunda, Production of silicon carbide from rice husks, J. Am. Ceram. Soc. 82 (6) (1999) 1393–1400.
[7] R. Liu, C. Zhang, X. Zhou, Y. Cao, Structural analysis of chemical vapor deposited β-SiC coatings from CH_3SiCl_3–H_2 gas precursor, J. Cryst. Growth 270 (1) (2004) 124–127.
[8] M. Valencia, V. Martínez, J. Cruz, Síntesis y caracterización de β-SiC, I Encuentro Nacional de Ciencia y Tecnología de Materiales, Módulo de Materiales Cerámicos, SIMAC, Universidad de Antioquia, 2004, pp. 1–11.

[9] M. Valencia, V. Martínez, J. Cruz, F. Chejne, Desarrollo de cerámicos avanzados obtenidos a partir de la cascarilla de arroz colombiana, IX Jornadas de Investigación, UPB, Medellín, 2004, pp. 135–143.

[10] J.M. Verteegen, et al. Concentration of silicon carbide with a density separation process, Miner. Metall. Process 7 (1990) 136–140.

[11] M. Filla, M. Chiappetta, Design and performance prediction of pyrolysis furnaces by flux methods and by the zone method, Comput. Chem. Eng. 3 (1) (1979) 527–534.

[12] R.V. Krishnarao, Effect of cobalt catalyst on the formation of SiC from rice husk silica-carbon black mixture, J. Mater. Sci. 30 (1995) 3645–3651.

[13] R.V. Krishnarao, Y.R. Mahajan, Effect of acid treatment on the formation of SiC whiskers from raw rice husk, J. Eur. Ceram. Soc. 15 (1995) 1229–1234.

[14] R.V. Krishnarao, M.M. Godkhindi, M. Chakraborty, Maximisation of SiC Whisker Yield During the Pyrolysis of Burnt Rice Husks, Chapman and Hall, UK, 1992, pp. 1227–1230.

[15] S.F. Moustafa, M.B. Morsi, A. Alm el Din, Formation of silicon carbide from rice husk, Canad. Metall. Q. 36 (5) (1997) 355–358.

[16] S.P. Lee, J.O. Jin, J.S. Park, A. Kohyama, Y. Katoh, H.K. Yoon, D.S. Bae, I.S. Kim, High temperature characterization of reaction sintered SiC based materials, J. Nucl. Mater. 329–333 (1) (2004) 534–538.

[17] B. Treviño, I. Gómez, V. Rodríguez, Obtención y caracterización de carburo y nitruro de silicio a partir de cascarilla de arroz, Ingenierías, Mexico, VI (19) (2003) 21–27.

[18] B.K. Padhi, C. Patnaik, Development of Si_2N_2O, Si_3N_4 and SiC ceramic materials using rice husk, Ceram. Int. 21 (1995) 213–220.

[19] R.V. Krishnarao, R. Mahajan, Formation of SiC whiskers from raw rice husk in argon atmosphere, Ceram. Int. 22 (1996) 353–358.

[20] V. Martínez, M. Valencia, J. Cruz, Compocasting process of cast Zamak particulate composites, Frontiers in Materials Research, A CIAM-CIMAT-CONICYT WORKSHOP, Viña del Mar, Chile, 26–29 April 2004, p. 68.

[21] G. Taguchi, Taguchi on Robust Technology Development: Bringing Quality Engineering Upstream, ASME Press, NY, 1993, pp. 63–74.